Two-channel Kondo problem in coupled interacting helical liquids

Sourav Biswas,[1] Alessandro De Martino,[2] Sumathi Rao,[3] and Arijit Kundu[1]

[1]*Department of Physics, Indian Institute of Technology - Kanpur, Kanpur 208 016, India.*
[2]*Department of Mathematics, City, University of London, EC1V 0HB London, UK*
[3]*International Centre for Theoretical Sciences (ICTS-TIFR),*
Shivakote, Hesaraghatta Hobli, Bangalore 560089, India
(Dated: June 26, 2023)

We study the two-channel Kondo problem in the context of two interacting helical liquids coupled to a spin-$\frac{1}{2}$ magnetic impurity. We show that the interactions between the two helical liquids significantly affect the phase diagram and other observable properties. Using a multichannel Luttinger liquid formalism, we analyze both the Toulouse limit, where an exact solution is available, and the weak coupling limit, which can be studied via a perturbative renormalization group (RG) approach. We recover the results for the 'decoupled' limit (interactions between the helical liquids switched off) and point out deviations from the known results due to this coupling. The model under study is mapped to a model of two effectively decoupled helical liquids coupled to an impurity. The perturbative RG study shows that each of these channels can flow to either a Ferromagnetic (FM) or an Anti-Ferromagnetic (AFM) fixed point. We obtain the phase diagram of the coupled system as a function of the system parameters. The observable consequences of the interaction between the two channels are captured using linear response theory. We compute the negative correction to the conductance due to the Kondo scattering processes and show how it scales with the temperature as a function of inter-channel interaction.

I. INTRODUCTION

Topological systems have been at the center of research in condensed matter physics due to their exotic properties, one of them being the existence of topologically protected boundary modes [1–3]. In the case of two-dimensional topological systems, these modes are robust one-dimensional channels. The quantum spin Hall insulators, for example, host helical channels at the edge of the sample by virtue of time-reversal symmetry (TRS) of the bulk Hamiltonian [4–6]. For the purpose of our study, we specifically focus on one-dimensional helical channels present in two-dimensional topological systems. We emphasize that the low energy regime of these systems is spanned by the states representing helical channels of one-dimensional nature.

A peculiarity of one dimension is that, in spite of the presence of Coulomb interaction, the system remains exactly solvable, under certain conditions. It is well understood that the interacting physics of these edge modes is described by the Luttinger liquid (LL) theory [7–9]. The applicability of the LL formalism can be attributed to the linear dispersion of the edge states at low energies and to the topological protection against various backscattering processes. However, such systems may not be exactly solvable in the presence of impurities. Here, we are interested to study the effect of a single magnetic impurity on the one-dimensional helical channels formed at the boundary of two-dimensional topological systems, taking Coulomb interaction into account. The LL formed by the helical channel in the presence of Coulomb interaction is termed helical liquid (HL).

It is well known that the Kondo effect describes the interaction between conduction electrons and a localized magnetic moment [10–15]. This phenomenon can also be investigated when Coulomb interaction is present in the conduction channel [16, 17]. So far, there have been studies addressing the problem of a spin-$\frac{1}{2}$ magnetic impurity coupled to a single helical liquid [18–21], as well as to two helical liquids [22–25]. In particular, Posske et al. [22] have studied the problem of two helical liquids decoupled from each other and coupled to a magnetic impurity. They have considered the Toulouse limit, where the model is exactly solvable, and have analyzed the behavior of the Kondo screening cloud.

Here, we study a model of two interacting helical liquids coupled to a spin-$\frac{1}{2}$ magnetic impurity, allowing for forward scattering processes between the two helical liquids which preserve the symmetries of the bare Hamiltonian. We show that the inclusion of all forward scattering processes allowed by symmetry modifies the properties of the system and has observable consequences. The model can be mapped to a model of two decoupled channels interacting with the impurity. For a specific set of parameters values (the so-called Toulouse point) the mapping is essentially an Emery-Kivelson [26] mapping, which reduces the interacting system to an exactly solvable two-channel resonant-level model [26–28]. Away from the Toulouse point, the mapping still works, but the model is no longer solvable. We then use perturbative renormalization group techniques to study the effects of the Kondo interaction. Perturbative RG techniques have been very instrumental in the study of Kondo effects [7, 10, 11]. One can use this technique to study the fixed points of the model, even though the model is not exactly solvable. One can further look into how these fixed points are modified as a function of system parameters. We note that previously the effect of scalar disorder has been studied in the context of a two channel Luttinger liquid set-up [29, 30] using the multichannel
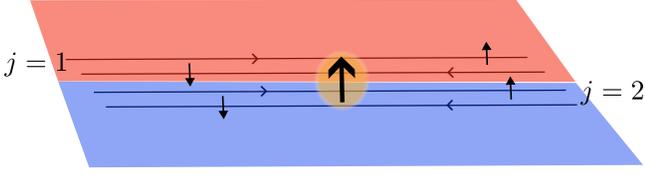
FIG. 1. Schematic picture of the system under study. Two helical liquids, labeled by the index $j = 1, 2$, propagate along the translational invariant direction $\hat{x}$. The right-moving fermions carry a spin up ($\uparrow$) index and the left-moving fermions a spin down ($\downarrow$) index. The two helical liquids are in close proximity to each other and are coupled to a spin-$\frac{1}{2}$ impurity, located at $x = 0$.

Luttinger liquid (MLL) formalism. Our analysis extends the study of impurities in a multichannel Luttinger liquid set-up to magnetic impurities as well.

The plan for the rest of the paper is as follows. In Sec. II, we introduce the model of two interacting helical liquids coupled to a spin-$\frac{1}{2}$ impurity. We diagonalize the interaction terms (without the impurity) and, by using unitary transformations, recast the coupling to the Kondo impurity into a simpler form. In Sec. III, we focus on the Toulouse point, where the model can be reduced to an exactly solvable one, and compute the impurity spectral function. In Sec. IV, we move away from the exactly solvable point and use the perturbative renormalization group (RG) method to obtain the Kondo temperatures for both channels and to study the fixed points as function of the system parameters. In Sec. V, we present the explicit form of the correlation to the conductance as a function of the temperature. Finally, in Sec. VI, we present our conclusions and provide an outlook. Throughout this paper, we set $\hbar = 1$.

II. MODEL

We consider a system of two interacting helical liquids coupled to a magnetic impurity expressed by the model Hamiltonian $H = H_{\mathrm{LL}} + H_{\mathrm{K}}$, where H_{LL} describes the bulk of the HLs and H_{K} represents a magnetic impurity coupled to the HLs. The bulk Hamiltonian takes the well-known form $H_{\mathrm{LL}} = H_0 + H_{\mathrm{int}}$, where H_0 is the bare part and H_{int} accounts for the Coulomb interaction present in the HLs. We begin by writing the bare part of the model as [4, 5, 7–9]

$$H_0 = -i \sum_{j,s} s v_j \int dx \, \Psi_{j,s}^\dagger \partial_x \Psi_{j,s}, \qquad (1)$$

where Ψ_{js} are the field operators for the jth channel, with $j \in \{1, 2\}$, and v_j are the Fermi velocities. We assume that the right-moving modes, denoted by $s = +$, carry spin up and the left-moving modes, denoted by $s = -$, carry spin down.

Next, we write down the interacting part of the model arising from the (screened) Coulomb interaction. We al-

low forward scattering processes between the two channels, which we write as

$$
\begin{aligned}
H_{\mathrm{int}} = \int dx \Big[& g_4^{(1)}(\rho_{1R}^2 + \rho_{1L}^2) + 2g_2^{(1)}\rho_{1R}\rho_{1L} + g_4^{(2)}(\rho_{2R}^2 \\
& + \rho_{2L}^2) + 2g_2^{(2)}\rho_{2R}\rho_{2L} + 2g_4^{(12)}(\rho_{1R}\rho_{2R} + \rho_{1L}\rho_{2L}) \\
& + 2g_2^{(12)}(\rho_{1R}\rho_{2L} + \rho_{1L}\rho_{2R}) \Big],
\end{aligned}
\tag{2}
$$

where $\rho_{j,s} = \Psi_{j,s}^\dagger \Psi_{j,s}$ is the fermionic density operator. Here g_2^ζ, g_4^ζ follow the standard g-ology convention with g_2^ζ denoting forward scattering processes involving density operators of movers in opposite directions and g_4^ζ denoting processes with movers in the same direction. The superscript $\zeta = 1, 2$ denotes scattering within individual channels $j = 1, 2$, whereas $\zeta = 12$ denotes scattering involving both channels. We note that the bare Hamiltonian H_0 is topologically protected and the terms included in Eq. (2) are allowed by TRS. In addition, these interacting liquids are coupled to a spin-$\frac{1}{2}$ impurity, with the Kondo Hamiltonian given by

$$
\begin{aligned}
H_{\mathrm{K}} = & \sum_{j,s} J_{z,j} s \Psi_{j,s}^\dagger(0)\Psi_{j,s}(0)\sigma^z \\
& + \sum_{j=1,2} J_{\perp,j}\Big(\Psi_{j,+}^\dagger(0)\Psi_{j,-}(0)\sigma^- + \mathrm{h.c.}\Big),
\end{aligned}
\tag{3}
$$

where $J_{z,j}$ and $J_{\perp,j}$ are the Kondo couplings for the jth channel, and σ^z, $\sigma^\pm = \sigma^x \pm i\sigma^y$ are the spin-$\frac{1}{2}$ operators for the impurity located at $x = 0$.

To proceed further, we employ the bosonization technique [31–33]. Since an HL has the same number of degrees of freedom as a spinless LL [18], two bosonic fields ϕ_j, θ_j are sufficient to bosonize the Hamiltonian H. We bosonize the fermion operator using the identity [31–33]

$$\Psi_{j,s} = (2\pi\xi_j)^{-1/2} e^{-i\sqrt{\pi}(\theta_j - s\phi_j)}, \tag{4}$$

where ξ_j is a microscopic cut-off length for channel j. The Klein factors have been neglected since they always appear in pairs in the quantities of interest we compute. We note that $\rho_{j,s} = \frac{1}{2\sqrt{\pi}}\partial_x(\phi_j - s\theta_j)$ and $\Pi_j = \partial_x\theta_j$. By combining the bosonized H_0 and H_{int}, we arrive at the multichannel Luttinger liquid (MLL) Hamiltonian

$$
\begin{aligned}
H_{\mathrm{LL}} = & H_0 + H_{\mathrm{int}} \\
= & \frac{1}{2}\int dx \Big(\partial_x \Phi^T M_\phi \partial_x \Phi + \partial_x \Theta^T M_\theta \partial_x \Theta \Big),
\end{aligned}
\tag{5}
$$

where we have used the notation $\Phi = (\phi_1 \;\; \phi_2)^T$, $\Theta = (\theta_1 \;\; \theta_2)^T$ and

$$M_\phi^{ij} = (v_i + \frac{g_4^{(i)} + g_2^{(i)}}{\pi})\delta_{ij} + \frac{g_4^{(12)} + g_2^{(12)}}{\pi}(1 - \delta_{ij}), \tag{6}$$

$$M_\theta^{ij} = (v_i + \frac{g_4^{(i)} - g_2^{(i)}}{\pi})\delta_{ij} + \frac{g_4^{(12)} - g_2^{(12)}}{\pi}(1 - \delta_{ij}). \tag{7}$$

We can now diagonalize H_{LL} using standard methods (see, e.g., [34, 35]). We assume that H_{LL} is diagonal in $\tilde{\Theta}$ and $\tilde{\Phi}$ fields, where $\tilde{\Phi} = (\tilde{\phi}_1 \ \ \tilde{\phi}_2)^T$, $\tilde{\Theta} = (\tilde{\theta}_1 \ \ \tilde{\theta}_2)^T$ and $\tilde{\Pi}_j = \partial_x \tilde{\theta}_j$. These fields are related to the Φ and Θ fields via linear transformations $\Phi = V_\phi \tilde{\Phi}$ and $\Theta = V_\theta \tilde{\Theta}$ such that $\tilde{\Theta}^T \tilde{\Phi} = \Theta^T \Phi$. The explicit forms of V_ϕ and V_θ are found to be

$$V_\phi = U_\phi^T D_\phi^{-\frac{1}{2}} \mathcal{U}^T \mathcal{D}^{\frac{1}{4}}, \tag{8}$$

$$V_\theta = U_\phi^T D_\phi^{\frac{1}{2}} \mathcal{U}^T \mathcal{D}^{-\frac{1}{4}}, \tag{9}$$

where U_ϕ is a matrix that diagonalizes M_ϕ of Eq. (6), D_ϕ is a diagonal matrix with the eigenvalues of M_ϕ as its diagonal entries. The orthogonal matrix $\mathcal{U}$ and the diagonal matrix $\mathcal{D}$ are obtained from the product of matrices $D_\phi^{\frac{1}{2}} U_\phi M_\theta U_\phi^T D_\phi^{\frac{1}{2}}$ by diagonalizing as $D_\phi^{\frac{1}{2}} U_\phi M_\theta U_\phi^T D_\phi^{\frac{1}{2}} = \mathcal{U}^T \mathcal{D} \mathcal{U}$. This procedure enables us to write the two-channel Luttinger liquid Hamiltonian $H_{\text{LL}} = H_0 + H_{\text{int}}$ as

$$H_{\text{LL}} = \sum_{j=1,2} \frac{u_j}{2} \int dx \left[(\partial_x \tilde{\theta}_j)^2 + (\partial_x \tilde{\phi}_j)^2 \right], \tag{10}$$

where the renormalized velocities u_j are the diagonal entries of $\mathcal{D}^{\frac{1}{2}}$. The Kondo Hamiltonian, in terms of the new fields, takes the form

$$H_{\text{K}} = \sum_{j=1,2} \left[-\frac{\tilde{J}_{z,j}}{\sqrt{\pi}} \tilde{\Pi}_j(0) \sigma^z \right.$$
$$\left. + \frac{J_{\perp,j}}{2\pi \xi_j} \left(e^{i2\sqrt{\pi}[V_\phi^{j1} \tilde{\phi}_1(0) + V_\phi^{j2} \tilde{\phi}_2(0)]} \sigma^+ + \text{h.c.} \right) \right], \tag{11}$$

where

$$\tilde{J}_{z,j} = \sum_{k=1,2} J_{z,k} V_\theta^{kj}. \tag{12}$$

At this point, we make a short digression to understand the decoupled limit from the calculations done so far. We notice that if we neglect the inter-channel interactions, $g_{2,4}^{(12)} = 0$, then $M_{\phi,\theta}$ are diagonal. Hence V_ϕ and V_θ are also diagonal and given by $V_\phi^{ij} = \sqrt{K_j} \delta_{ij}$ and $V_\theta^{ij} = \delta_{ij}/\sqrt{K_j}$, where

$$K_j = \sqrt{1 + \frac{g_4^{(j)} - g_2^{(j)}}{\pi v_j}} \Big/ \sqrt{1 + \frac{g_4^{(j)} + g_2^{(j)}}{\pi v_j}}$$

is the usual Luttinger liquid parameter for channel j. Therefore, $\tilde{\phi}_j = \phi_j/\sqrt{K_j}$, $\tilde{\Pi}_j = \sqrt{K_j} \Pi_j$, $u_j = v_j/K_j$, and $\tilde{J}_{z,j} = J_{z,j}/\sqrt{K_j}$, and we recover the Hamiltonian considered in [22, 24].

The Hamiltonian (10) describes two effectively decoupled HLs obtained by the diagonalization procedure when $g_{2,4}^{(12)} \neq 0$. The new decoupled fields $\tilde{\phi}_j$ have been used to rewrite the Kondo Hamiltonian. We observe from

Eq. (11) that both fields $\tilde{\phi}_1$ and $\tilde{\phi}_2$ appear in each of the exponential terms of H_{K}. This is a manifestation of the finite inter-channel scattering processes $g_{2,4}^{(12)}$. Hence, even if H_{LL} can be cast into a diagonal form, the Kondo Hamiltonian still couples the two fields. We proceed further to reduce the full Hamiltonian H to a Hamiltonian describing two decoupled interacting channels coupled to a single Kondo impurity, by devising a unitary transformation $U_{\text{d}} = e^{i2\sqrt{\pi}(\lambda_1 \tilde{\phi}_1(0) + \lambda_2 \tilde{\phi}_2(0))\sigma^z}$ and choosing $\lambda_{1,2}$ appropriately to arrive at $\tilde{H} \equiv U_{\text{d}} H U_{\text{d}}^\dagger$ given by

$$\tilde{H} = \sum_{j=1,2} \left[\frac{u_j}{2} \int dx \left[\tilde{\Pi}_j^2 + (\partial_x \tilde{\phi}_j)^2 \right] \right.$$
$$\left. - \frac{\tilde{J}'_{z,j}}{\sqrt{\pi}} \tilde{\Pi}_j(0) \sigma^z + \frac{J_{\perp,j}}{2\pi \xi_j} \left(e^{i2\sqrt{\pi}\kappa_j \tilde{\phi}_j(0)} \sigma^+ + \text{h.c.} \right) \right], \tag{13}$$

where

$$\kappa_j = V_\phi^{jj} - V_\phi^{\bar{j}j} \quad \text{and} \quad \tilde{J}'_{z,j} = \tilde{J}_{z,j} - 2\pi u_j V_\phi^{\bar{j}j}. \tag{14}$$

Here, $\bar{j} = 2, 1$ for $j = 1, 2$. We refer to App. A for the details of the derivation. We use this Hamiltonian in Sec. IV to derive the RG flow of the Kondo couplings.

Alternatively, we can use the unitary transformation to cancel the $\tilde{J}_{z,j}$-terms. This is accomplished by setting $\lambda_j = -\frac{\tilde{J}_{z,j}}{2\pi u_j}$, as shown in App. A. We then arrive at

$$\tilde{H} = \sum_{j=1,2} \left[\frac{u_j}{2} \int dx \left[\tilde{\Pi}_j^2 + (\partial_x \tilde{\phi}_j)^2 \right] \right.$$
$$\left. + \frac{J_{\perp,j}}{2\pi \xi_j} \left(e^{i2\sqrt{\pi} \sum_k \kappa_{jk} \tilde{\phi}_k(0)} \sigma^+ + \text{h.c.} \right) \right], \tag{15}$$

where we have defined

$$\kappa_{jk} = V_\phi^{jk} - \frac{\tilde{J}_{z,k}}{2\pi u_k}. \tag{16}$$

This Hamiltonian is the starting point for the calculation of observables. In the next section, we study a particular limit in which $H = H_{\text{LL}} + H_{\text{K}}$ is exactly solvable, and in Sec. IV we use the perturbative RG approach to study the weak coupling limit beyond the solvable point.

Before moving on, we briefly comment on the nonlinear terms that have been omitted in the interacting Hamiltonian. In general, the inclusion of interaction-induced backscattering operators can open a gap and render the gapless Luttinger liquid physics invalid. However, a helical liquid is topologically protected against intra-channel backscattering terms. We consider here a regime in which also the inter-channel backscattering terms are negligible [9]. Furthermore, we assume that the system is away from half-filling and neglect all Umklapp processes [9], as further discussed in App. B. In the same appendix, we also show that the Kondo spin-flip scattering involving two different channels becomes irrelevant under certain

conditions imposed on the system parameters. We only take into account the Kondo spin-flip scatterings within the same channel, assuming that the aforementioned irrelevance is satisfied.

III. EXACTLY SOLVABLE POINT

In this section, we show that for special values of the system parameters the model admits an exact solution [26, 38]. In fact, for the Hamiltonian (15), there are two possible sets of conditions under which the mapping can be achieved. The first set of conditions is

$$\kappa_{11} = \kappa_{22} = 0, \qquad \kappa_{12}^2 = \kappa_{21}^2 = \frac{1}{2}. \qquad (17)$$

The first condition ensures that the two channels decouple, i.e., only one field appears in each exponential operator in the Kondo interaction. The second ensures that the Kondo interaction has the scaling dimension of a fermionic field. Using Eq. (16), this set of conditions can be written in terms of V_ϕ and $\tilde{J}_{z,j}$ as

$$\tilde{J}_{z,1} = 2\pi u_1 V_\phi^{11}, \quad \tilde{J}_{z,2} = 2\pi u_2 V_\phi^{22}, \qquad (18)$$

$$(V_\phi^{11} - V_\phi^{21})^2 = (V_\phi^{22} - V_\phi^{12})^2 = \frac{1}{2}. \qquad (19)$$

These conditions can only be satisfied when V_ϕ is a non-diagonal matrix. When these conditions hold, the two-channel Kondo problem can be mapped to a resonant-level problem [26–28]. We can find out the solution in terms of the system parameters, using the definition of V_ϕ.

Note that the alternative choice

$$\kappa_{12} = \kappa_{21} = 0, \qquad \kappa_{11}^2 = \kappa_{22}^2 = \frac{1}{2} \qquad (20)$$

becomes

$$\tilde{J}_{z,1} = 2\pi u_1 V_\phi^{21}, \quad \tilde{J}_{z,2} = 2\pi u_2 V_\phi^{12}, \qquad (21)$$

$$(V_\phi^{11} - V_\phi^{21})^2 = (V_\phi^{22} - V_\phi^{12})^2 = \frac{1}{2}. \qquad (22)$$

We see that Eq. (22) is precisely the same as Eq. (19). Both choices lead to the reduction of Eq. (15) to a resonant-level model with two non-interacting channels coupled to a single magnetic impurity. Since the exact solution depends on relationships between different parameters of the model, it is clear that as the parameter values change, it is only for certain values that we will get an exact solution. In Fig. 2 we plot the two conditions $(V_\phi^{11} - V_\phi^{21})^2 - \frac{1}{2} \equiv V_{sol}^1 = 0$ and $(V_\phi^{22} - V_\phi^{12})^2 - \frac{1}{2} \equiv V_{sol}^2 = 0$ as a function of two parameters at a time (the other parameters have been fixed at the values given in Table I). Then, the intersections of the curves $V_{sol}^1 = 0$ and $V_{sol}^2 = 0$ give the points where an exact solution is possible. As discussed in the previous section, one has to

choose the parameters in a way such that Eq. (15) is sufficient to describe all possible scattering processes. Following the analysis done in App. B, we make the choice of the parameters in a way such that

$$\frac{1}{4} \sum_{j=1,2} \left(V_\theta^{1j} - V_\theta^{2j} \right)^2 + \frac{1}{4} \sum_{j=1,2} \left(V_\phi^{1j} \mp V_\phi^{2j} \right)^2 > 1. \quad (23)$$
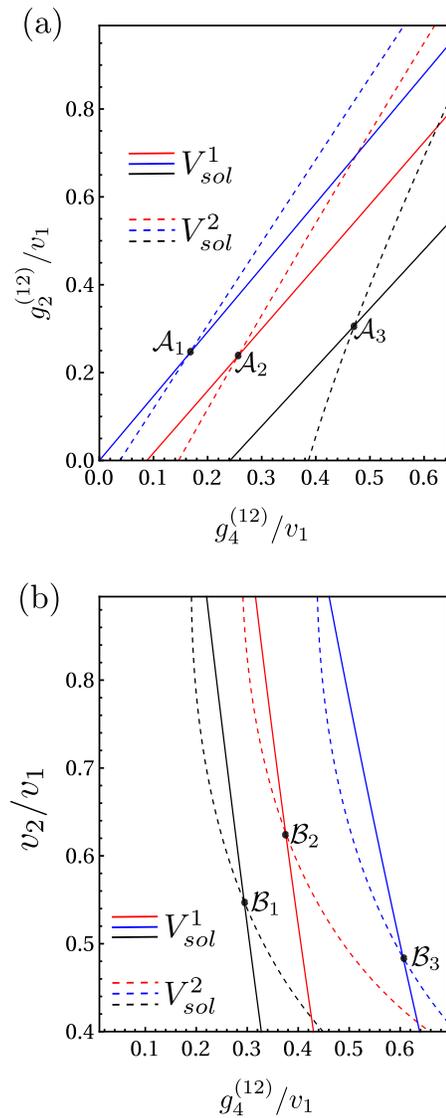

FIG. 2. Two lines given by $V_{sol}^1 = 0$ and $V_{sol}^2 = 0$ are plotted as a function of system parameters. The intersection of these two lines denotes an exactly solvable point, where the model can be transformed into a model of two non-interacting channels coupled to a single impurity. These intersections are denoted by separate symbols $\mathcal{A}_j$ and $\mathcal{B}_j$. Changing the system parameters shifts the exact solution. In (a) we have varied $g_2^{(12)}$ and $g_4^{(12)}$. The origin corresponds to the decoupled limit of the problem. In (b), v_2 and $g_4^{(12)}$ are varied. All the parameters are scaled by v_1. The other parameters which are required to generate this plot are listed in Table. I.

	v_2/v_1	$g_2^{(1)}/v_1$	$g_2^{(2)}/v_1$	$g_4^{(1)}/v_1$	$g_4^{(2)}/v_1$	$g_2^{(12)}/v_1$	$g_4^{(12)}/v_1$
$\mathcal{A}_1$	1.5	$2.0\,\pi$	$2.4\,\pi$	2.2π	2.5π	...	...
$\mathcal{A}_2$	0.5	1.25π	1.4π	1.4π	1.5π	...	...
$\mathcal{A}_3$	0.4	1.2π	1.4π	1.6π	1.5π	...	...
$\mathcal{B}_1$	...	1.45π	1.475π	1.6π	1.6π	0.35	...
$\mathcal{B}_2$	...	1.45π	1.475π	1.5π	1.5π	0.5	...
$\mathcal{B}_3$	...	1.45π	1.65π	1.6π	1.75π	0.75	...

TABLE I. Values of the system parameters used in Fig. 2. The blank boxes with dots stand for the parameters which are varied in the plots.

The choice of the parameters for the mapping to the resonant level model has been made in a way such that the vertex operator, $e^{i2\sqrt{\pi}\sum_k \kappa_{jk}\tilde{\phi}_k(0)}$ can be refermionized using the same bosonization identity that we used earlier so that the model reduces to that of free fermions. We can write the non-chiral boson fields used for describing the HL as $\tilde{\phi}_j = (\tilde{\phi}_{j,L} + \tilde{\phi}_{j,R})$ and $\tilde{\theta}_j = (\tilde{\phi}_{j,L} - \tilde{\phi}_{j,R})$ where R and L denote the right and left movers. In order to cast the Hamiltonian as an exactly solvable non-interacting fermion model, we first focus on the Luttinger liquid defined on the positive and negative x-axis, separately. The system on the right and left half-lines is "unfolded" [26, 31, 39] so that the Hamiltonian is presented in a chiral form. We follow the convention of writing $\tilde{\phi}_{j,R}(x)$ and $\tilde{\phi}_{j,L}(x)$ fields defined on the positive x-axis in terms of $\tilde{\phi}_{j,R}^e(x)$ and $\tilde{\phi}_{j,R}^e(-x)$ fields defined on the full x-axis. This is done as follows: $\tilde{\phi}_{j,R}^e(x) = \tilde{\phi}_{j,R}(x)$ and $\tilde{\phi}_{j,R}^e(-x) = \tilde{\phi}_{j,L}(x)$. One can obtain two chiral liquids in the bulk of the channel using these identities. Then, one must identify the chiral boson fields to be equal at $x = 0$ i.e. $\tilde{\phi}_{j,L}^e(0) = \tilde{\phi}_{j,R}^e(0)$. We notice that the Kondo scattering term is defined only at $x = 0$. We choose one chiral field out of $\tilde{\phi}_{j,R}^e(0)$ and $\tilde{\phi}_{j,L}^e(0)$, to write the vertex operator of the Kondo interaction term. After doing so, the Hamiltonian can again be written on the full line in terms of chiral fields only. However, depending on the choice of the chiral field used to write down the vertex operator in the Kondo scattering term, one chiral field remains decoupled from the impurity and can be discarded from the resonant level model. In what follows, we use the right-moving bosonic field to write down the exact solution. The bosonization identity $\Psi_j = (2\pi\xi_j)^{-1/2}e^{i2\sqrt{\pi}\tilde{\phi}_{j,R}^e}$ can be used to write the model in terms of fermions. In this limit, Eq. (15) can be expressed in terms of chiral spinless fermions $\Psi_j(x)$ [19] as

$$H_{\mathrm{T}} = \sum_j \left[-iu_j \int dx\, \Psi_j^\dagger(x)\partial_x \Psi_j(x) + \epsilon_d d^\dagger d \right.$$
$$\left. + \frac{J_{\perp,j}}{\sqrt{2\pi\xi_j}} \left(d^\dagger \Psi_j(0) + \Psi_j^\dagger(0)d \right) \right], \tag{24}$$

where the impurity spin residing at $x = 0$ has been modeled by a discrete level, such that $\sigma_z = d^\dagger d - 1/2$. The operator $d^\dagger$ creates a spinless fermion in the discrete level and ϵ_d is the chemical potential at the site of the discrete level. We refer to App. C for the details of the exact solution. At the exactly solvable point, one can self-consistently compute the energy spectrum and the impurity spectral function [40]. In our case, the spectral function turns out to be a Lorentzian with a level width $\Gamma = \sum_j \frac{J_{\perp,j}^2}{4\pi\xi_j u_j}$. We see that the two contributions coming from the two independent channels add up directly.

In the decoupled limit (which can be obtained by switching off the interchannel forward scattering processes $g_{2,4}^{(12)}$), our result matches with one of the exactly solvable points derived in [22]. In this limit, $M_{\phi,\theta}$ are diagonal and $K_j = \kappa_j^2 = (V_\phi^{jj})^2$. We have chosen $\kappa_j = 1/\sqrt{2}$ and as a result $K_1 + K_2 = 1$. We note that our exact solution does not require the channels to have equal velocities. In fact, due to the presence of off-diagonal terms in $M_{\phi,\theta}$, the renormalized velocities of the diagonalized Hamiltonian are not equal in our case. At the exactly solvable point choosing $K_j = 1$ leads to an effectively non-interacting fermionic model coupled to magnetic impurity, if inter-channel processes are switched off. This particular limit is not of our interest. However we note, this would lead to another exactly solvable limit derived in [22].

IV. BEYOND THE EXACTLY SOLVABLE LIMIT

In this section, we use the perturbative renormalization group technique to analyze the flow of the Kondo couplings [41, 42]. By using the effectively decoupled Hamiltonian in Eq. (13), we find that for each channel j the RG equations (up to second order in the couplings) are given by

$$\frac{d\tilde{J}_{z,j}'}{dl} = \nu_j \kappa_j^3 J_{\perp,j}^2, \tag{25}$$

$$\frac{dJ_{\perp,j}}{dl} = (1 - \kappa_j^2)J_{\perp,j} + \nu_j \kappa_j \tilde{J}_{z,j}' J_{\perp,j}, \tag{26}$$

where $\nu_j \equiv \frac{1}{\pi u_j}$ [?]. We emphasize that the MLL formalism is instrumental in mapping the results to a form similar to the known one-channel counterpart [7, 18, 41]. The details of the derivation are provided in the App. D. The equations (25) and (26) can be put in a more compact form by defining $\nu_j \bar{J}_{z,j} = \nu_j \kappa_j \tilde{J}_{z,j}' + 1 - \kappa_j^2$ as

$$\frac{d\bar{J}_{z,j}}{dl} = \nu_j \kappa_j^4 J_{\perp,j}^2, \tag{27}$$

$$\frac{dJ_{\perp,j}}{dl} = \nu_j \bar{J}_{z,j} J_{\perp,j}. \tag{28}$$

The trajectories of the flow equations are given by $(\kappa_j^2 J_{\perp,j})^2 - (\bar{J}_{z,j})^2 = c$, where c is a constant. It is known that a single channel either flows to an anti-ferromagnetic
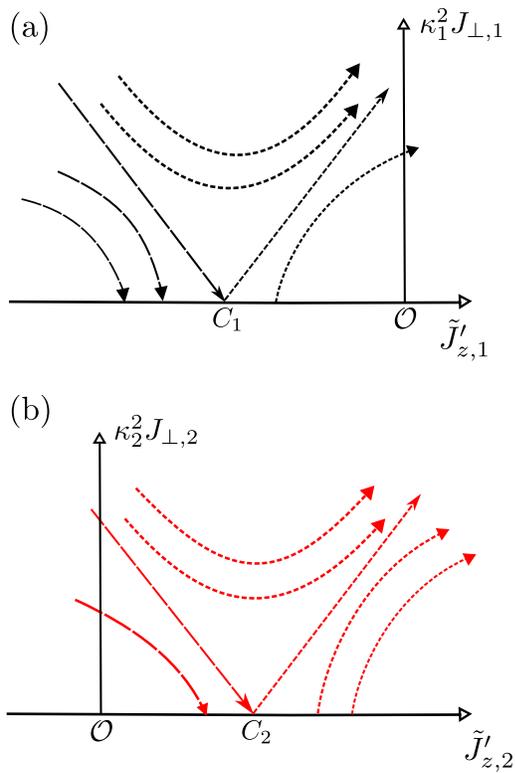
FIG. 3. Schematic representation of the RG flow in Eqs. (27) and (28). In panel (a) and (b) we show two sets of flow trajectories pertaining to the two different channels. The symbol $\mathcal{O}$ denotes the point $(J_{\perp,j}, \tilde{J}'_{z,j}) = (0,0)$. The position of the starting point of the trajectory relative to C_j (rather than to $\mathcal{O}$) determines whether the system flows to a FM or an AFM fixed point.

(AFM) or a ferromagnetic (FM) fixed point (FP) [10, 18]. Earlier works have shown how the RG flow in such a system depends on the Luttinger parameter [7, 18]. In our case, each of the effectively decoupled channels behaves like a single Luttinger liquid wire and can flow to either FM- or AFM-FP separately. However, the inclusion of inter-channel interactions in Eq. (2) modifies the range of parameters of the system for which the couplings flow either to the FM or the AFM fixed point.

We plot a schematic flow diagram pertaining to the above RG equations in Fig. 3. If the Kondo couplings of channel j of Eq. (13) flow to infinity, then the impurity is strongly coupled to channel j. On the other hand, if $J_{\perp,j}$ renormalizes to zero, then the impurity is weakly coupled with channel j. The transition point C_j separates the $\tilde{J}'_{z,j}$ axis into two portions having opposite flows. To study different FPs, we choose $J_{\perp,j} = 0$ of Fig. 3 as the initial condition. On this line, whether the system flows to FM or AFM fixed point is decided by the position of C_j.

In Fig. 3, the position of the transition point C_j on $\tilde{J}'_{z,j}$ axis depends on the solution of $\nu_j \kappa_j \tilde{J}'_{z,j} + 1 - \kappa_j^2 = 0$. We know from Eq. (14) that $\kappa_j = V_\phi^{jj} - V_\phi^{\bar{j}j}$. Hence, we see that inter-channel interactions shift the position of
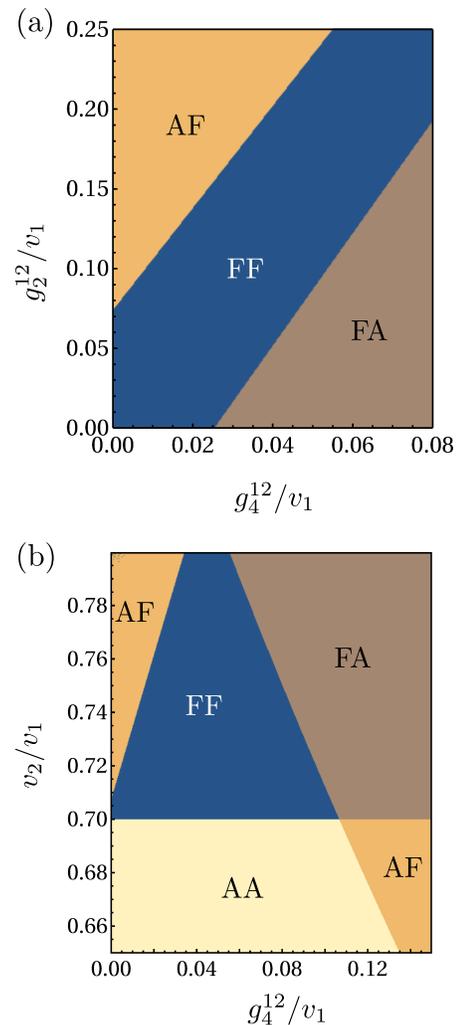

FIG. 4. The above diagrams show the different FPs to which the two channels flow, as a function of the system parameters. We refer to these diagrams of the parameter space as phase diagrams. Each of the effectively decoupled channels can flow to either the A or the F fixed point, starting from $J_{\perp,j} = 0$, (see the discussion in the main text). In panel (a) we set $v_2/v_1 = 0.75$, $g_2^{(1)}/v_1 = 0.65\pi$, $g_2^{(2)}/v_1 = 0.7\pi$, $g_4^{(1)}/v_1 = 1.275\pi$, $g_4^{(2)}/v_1 = 1.5\pi$. In panel (b) we set $g_2^{(1)}/v_1 = 0.5\pi$, $g_2^{(2)}/v_1 = 0.6\pi$, $g_4^{(1)}/v_1 = 1.2\pi$, $g_4^{(2)}/v_1 = 1.4\pi$, $g_2^{(12)}/v_1 = 0.175$.

the transition point on $\tilde{J}'_{z,j}$ axis. As long as $\kappa_j \neq 1$ the transition point does not lie at $\tilde{J}'_{z,j} = 0$ which we denote by $\mathcal{O}$.

Next, we look into the RG flow of each of the effectively decoupled channels of Eq. (13). It is easy to identify, from Fig. 3(b), that for $\kappa_2 > \kappa_2^{-1}$ there is a region on the positive $\tilde{J}'_{z,2}$ axis between C_2 and $\mathcal{O}$, where even if the Kondo coupling is positive i.e. AFM like, the system flows to an FM fixed point. We denote these fixed points by F. By the same token, a channel can flow to an AFM FP despite being expected to flow to an FM FP. Such FPs are denoted by A. For example in Fig. 3(a), the transition

point C_1 lies to the left of $\mathcal{O}$ and FPs of type A are obtained for the choice $\kappa_1 < \kappa_1^{-1}$. We can combine these FPs of both channels and name them '$\mathcal{P}_j \mathcal{P}_{j'}$', where $\mathcal{P}_j$ denotes the FP of channel j and can be either A or, F. Once we have identified the fixed points we can study their dependence on different parameters, as shown in Fig. 4. The phase diagrams in Fig. 4 are representations of the parameter space of the Hamiltonian, where different fixed points are reached in different segments of the parameter space. These parameters have to be chosen in a way such that conditions written down in Eq. (23) are satisfied. We note that a similar analysis can also be done for different choices of $J_{\perp,j}$, as an initial condition.

The characteristic feature of an FM FP is the renormalization of $J_{\perp,j}$ to zero. We note that the spin-flip scattering processes are governed by this coupling and as a result, in an FM FP no strongly coupled bound state formation takes place between the conduction electron and the impurity spin. Another way to understand this is that, if $J_{\perp,j}$ flows to zero then the conduction electrons of channel j do not take part in spin-flip Kondo scattering processes. However, if $J_{\perp,j}$ flows to infinity, then the electrons of the effectively decoupled channel (j) participate in spin-flip scattering processes leading to the formation of a bound state between the electron of channel j and the impurity spin. This is a feature of AFM FP. Thus, in either AF or FA phase, there is only one channel that contributes to bound state formation. This bound state is a spin singlet and in these two phases, the impurity is screened. In the FF phase, none of the channels are strongly coupled with the impurity and hence there is no screening. In the AA phase, both channels try to couple anti-ferromagnetically and as a consequence overscreening of the impurity can take place. One should keep in mind that the phenomenon of overscreening is extremely sensitive to the anisotropy of the Kondo coupling and is only expected to be observed for isotropic coupling [12]. For an anisotropic case, the channel with the larger value of Kondo coupling would win over the other channel and form a singlet.

From Eqs. (25) and (26), we can calculate the Kondo temperature for the two channels. We define $\alpha^j = \sqrt{(\tilde{J}'_{z,j,0})^2/(J_{\perp,j,0})^2 - 1}$, where $\tilde{J}'_{z,j,0}, J_{\perp,j,0}$ are the bare values of the $\tilde{J}'_{z,j}, J_{\perp,j}$ couplings. With Λ being the bandwidth of the original system, the Kondo temperature T_K^j for channel j is given by

$$T_K^j = \Lambda \exp\Big(-\frac{\sinh^{-1}(\alpha_j)}{\alpha_j \nu_j J_{\perp,j,0}}\Big). \tag{29}$$

We note that T_K^j is the characteristic energy scale of the Kondo effect pertaining to each of these channels.

V. OBSERVABLE CONSEQUENCE

The Kondo effect gives rise to a negative correction, $\delta\mathcal{G}(\omega)$, to the conductance of the HLs, originating from spin-flip scattering processes mediated by the magnetic impurity. This correction vanishes for HLs as temperature $T \to 0$ and also in the DC limit when frequency $\omega \to 0$ [18, 19]. However, the signature of Kondo scattering can still be captured by computing the correction at non-zero T and ω. In order to study the scaling of the correction to the conductance, one can compute $\delta\mathcal{G}(\omega)$ by incorporating a difference of chemical potential between the right and left movers, respectively. This is equivalent to computing $\delta\mathcal{G}(\omega)$ from the spin-flip current obtained by introducing an effective magnetic field which creates an energy difference between the spin up and the spin down components of the impurity [19, 21]. We assume weak backscattering by the impurity such that $\delta\mathcal{G}(\omega) \ll e^2$ where e is the electron charge.

Following [19], we attach $H_\mathcal{V} = -e\mathcal{V}\sigma^z$ to the Hamiltonian of Eq. (15) and compute transport properties in response to the spin-flip current using $H_\mathcal{V}$. One can use the Kubo formula [19, 21, 40] to compute this correction. The details of the calculation, including the general form of the correction, are given in App. E. One can write down the exact expressions for the conductance correction in the limit $J_{\perp,j}^2 \ll \omega \ll T$. The temperature scaling of $\delta\mathcal{G}$ is given by

$$\delta\mathcal{G} = \mathcal{L}_1 T^{2(\kappa_{11}^2 + \kappa_{12}^2)-2} + \mathcal{L}_2 T^{2(\kappa_{21}^2 + \kappa_{22}^2)-2} + \mathcal{L}_3 T^{2(\kappa_{11}\kappa_{12} + \kappa_{22}\kappa_{21})-2}, \tag{30}$$

where

$$\mathcal{L}_1 = -\frac{e^2}{4}\left(\frac{J_{\perp,1}}{2\pi\xi_1}\right)^2 \left(\frac{2\pi}{\Lambda}\right)^{2\kappa_{11}^2} \left(\frac{2\pi}{\Lambda}\right)^{2\kappa_{12}^2} \left(\frac{1}{\pi}\right)^2 \frac{\pi\Gamma(\kappa_{11}^2 + \kappa_{12}^2)^2}{\Gamma(2(\kappa_{11}^2 + \kappa_{12}^2))}, \tag{31}$$

$$\mathcal{L}_2 = -\frac{e^2}{4}\left(\frac{J_{\perp,2}}{2\pi\xi_2}\right)^2 \left(\frac{2\pi}{\Lambda}\right)^{2\kappa_{21}^2} \left(\frac{2\pi}{\Lambda}\right)^{2\kappa_{22}^2} \left(\frac{1}{\pi}\right)^2 \frac{\pi\Gamma(\kappa_{21}^2 + \kappa_{22}^2)^2}{\Gamma(2(\kappa_{21}^2 + \kappa_{22}^2))}, \tag{32}$$

$$\mathcal{L}_3 = -\frac{e^2}{2}\frac{J_{\perp,1}J_{\perp,2}}{(2\pi)^2\xi_1\xi_2} \left(\frac{2\pi}{\Lambda}\right)^{2(\kappa_{11}\kappa_{12})} \left(\frac{2\pi}{\Lambda}\right)^{2\kappa_{22}\kappa_{21}} \left(\frac{1}{\pi}\right)^2 \frac{\pi\Gamma(\kappa_{11}\kappa_{12} + \kappa_{22}\kappa_{21})^2}{\Gamma(2(\kappa_{11}\kappa_{12} + \kappa_{22}\kappa_{21}))}. \tag{33}$$

The result takes a form similar to the known case of one HL coupled to a Kondo impurity [18, 19]. We notice that,

at the exactly solvable point, the integral from which $\mathcal{L}_3$ is obtained, goes to zero, as discussed in App. E and one is left with $\mathcal{L}_1$ and $\mathcal{L}_2$. The assumed limit for the above expression is important, as we see that at high temperature (i.e. $T \gg \omega \gg J^2_{\perp,j}$) the Kondo scattering gives rise to a negative correction, implying deviation from standard scaling of the conductance in HLs in the absence of Kondo impurity. We also see that in this limit the correction is independent of ω.

VI.   CONCLUSION

In this paper, we have presented a general framework for studying two interacting helical liquids coupled to a Kondo impurity, including both intra-channel as well as inter-channel interactions.

We have derived the conditions under which an exact solution of the model can be obtained with the additional restriction of $\kappa_j = 1/\sqrt{2}$, where κ_j is defined in Eq. (14). This solvable point has been calculated using an Emery-Kivelson type of transformation. We have included inter-channel forward scattering processes yielding exact solutions to the problem examined beyond the scenarios captured by Refs. [22, 26, 38]. In Sec. III we have shown how the exact solutions of the decoupled limit (obtained by switching off $g^{12}_{2,4}$) can be derived from our calculation. At the solvable point, we have calculated the spectral function. We have shown that the level width is the sum of contributions coming from each channel. The spectral function has experimental significance in many systems; for example, quantum dots show the Kondo effect where the hallmark of Kondo physics is the differential conductance which is proportional to the spectral function [43–46].

We have studied the model away from the exactly solvable point, by mapping it to a pair of effectively decoupled HLs interacting with a single magnetic impurity,

as derived in Eq. (13). By using a perturbative RG approach, we have shown that these two renormalized channels can separately flow to either the FM or the AFM fixed point. Here, the AFM fixed point indicates the formation of a bound state between the conduction electron and impurity spin, whereas the FM fixed point means the absence of the same, although a finite residual coupling can be present in the FM case. In Fig. 3 we show a schematic flow diagram pertaining to the RG equations derived in Sec. IV. The phase diagrams obtained from our RG analysis are shown in Fig. 4. As noted earlier, these phase diagrams represent the parameter space of the Hamiltonian where the effectively decoupled HLs reach different FPs in different segments of the diagram. In Sec. IV, we also have discussed the nature of the impurity screening at different fixed points. In the FF phase, there is no singlet formation due to the absence of screening. In the FA and AF phases, the impurity is screened and in the AA phase, the impurity is either screened or overscreened depending on anisotropy in Kondo couplings. In Sec. V, we have presented a study of the linear response of the system in the weak coupling limit. We have shown that the Kondo effect gives rise to a negative correction to the conductance of the HLs. The temperature scaling of this correction as a function of system parameters has been shown explicitly.

VII.   ACKNOWLEDGEMENT

Appendix A: Unitary transformations

Under the action of the unitary transformation

$$U = e^{i2\sqrt{\pi}(\lambda_1 \tilde{\phi}_1(0) + \lambda_2 \tilde{\phi}_2(0))\sigma^z}, \tag{A1}$$

the Luttinger liquid Hamiltonian H_{LL} transforms as

$$H_{\mathrm{LL}} \to \tilde{H}_{\mathrm{LL}} = U H_{\mathrm{LL}} U^\dagger = \sum_{j=1,2} \left[\frac{u_j}{2} \int dx \left[\tilde{\Pi}_j^2 + (\partial_x \tilde{\phi}_j)^2 \right] - 2\sqrt{\pi} \lambda_j u_j \tilde{\Pi}_j(0)\sigma^z \right], \tag{A2}$$

while the Kondo Hamiltonian H_{K} transforms as

$$H_{\mathrm{K}} \to \tilde{H}_{\mathrm{K}} = U H_{\mathrm{K}} U^\dagger = \sum_{j=1,2} \left[-\frac{\tilde{J}_{z,j}}{\sqrt{\pi}} \tilde{\Pi}_j(0)\sigma^z + \frac{J_{\perp,j}}{2\pi\xi_j} \left(e^{i2\sqrt{\pi}[(V_\phi^{j1} + \lambda_1)\tilde{\phi}_1(0) + (V_\phi^{j2} + \lambda_2)\tilde{\phi}_2(0)]}\sigma^+ + \mathrm{h.c.} \right) \right]. \tag{A3}$$

(We have omitted an unimportant constant.) We then arrive at a decoupled-channel Hamiltonian with either of the two following choices:

$$\lambda_j = -V_\phi^{jj} \quad \text{or} \quad \lambda_j = -V_\phi^{\bar{j}j}. \tag{A4}$$

(We use the notation $\bar{j} = 2, 1$ for $j = 1, 2$). We select the second option, and collecting $\tilde{H}_{\text{LL}}$ and $\tilde{H}_{\text{K}}$, we arrive at the Hamiltonian

$$\tilde{H} = \sum_{j=1,2} \left[\frac{u_j}{2} \int dx \left[\tilde{\Pi}_j^2 + (\partial_x \tilde{\phi}_j)^2 \right] - \frac{\tilde{J}'_{z,j}}{\sqrt{\pi}} \tilde{\Pi}_j(0) \sigma^z + \frac{J_{\perp,j}}{2\pi\xi_j} \left(e^{i2\sqrt{\pi}\kappa_j \tilde{\phi}_j(0)} \sigma^+ + \text{h.c.} \right) \right], \tag{A5}$$

where we have defined

$$\tilde{J}'_{z,j} = \tilde{J}_{z,j} - 2\pi u_j V_\phi^{\bar{j}j}, \quad \kappa_j = V_\phi^{jj} - V_\phi^{\bar{j}j}. \tag{A6}$$

We use this Hamiltonian for the calculation of the RG flow of the Kondo couplings in Sec. IV and App. D.

Alternatively, in the unitary transformation (A1) we can set $\lambda_j = -\frac{\tilde{J}_{z,j}}{2\pi u_j}$ and we obtain

$$\tilde{H} = \sum_{j=1,2} \left[\frac{u_j}{2} \int dx \left[\tilde{\Pi}_j^2 + (\partial_x \tilde{\phi}_j)^2 \right] + \frac{J_{\perp,j}}{2\pi\xi_j} \left(e^{i2\sqrt{\pi}\sum_k \kappa_{jk}\tilde{\phi}_k(0)} \sigma^+ + \text{h.c.} \right) \right], \tag{A7}$$

where we have defined

$$\kappa_{jk} = V_\phi^{jk} - \frac{\tilde{J}_{z,k}}{2\pi u_k}. \tag{A8}$$

We employ this form of the Hamiltonian in the discussion of the solvable point in Sec. III and for the perturbative calculation of the correction to the conductance in Sec. V.

Appendix B: Interaction Hamiltonian

In this appendix we establish the conditions under which it is justified to retain only the interaction terms included in Eq. (2). Following [9], the interaction Hamiltonian for a two-channel HL in general comprises terms that lead to nonlinearities in the bosonized theory. These terms include the Umklapp scattering processes

$$\Psi_{j\uparrow}^\dagger(x)\Psi_{j\uparrow}^\dagger(x+a)\Psi_{j\downarrow}(x+a)\Psi_{j\downarrow}(x)e^{-i4k_F x} + \text{h.c.}, \quad j = 1, 2. \tag{B1}$$

We omit these processes on account of the fact that we consider the generic incommensurate situation, i.e., $4k_F$ different from a reciprocal lattice vector.

Next, let us consider Kondo scatterings between different channels. They are described by the following operators:

$$\Psi_{1,\uparrow}^\dagger \Psi_{2,\uparrow} - \Psi_{1,\downarrow}^\dagger \Psi_{2,\downarrow} \sim e^{i\sqrt{\pi}((V_\theta^{11}-V_\theta^{21})\tilde{\theta}_1+(V_\theta^{12}-V_\theta^{22})\tilde{\theta}_2)} \sin(\sqrt{\pi}((V_\phi^{11}-V_\phi^{21})\tilde{\phi}_1+(V_\phi^{12}-V_\phi^{22})\tilde{\phi}_2)), \tag{B2}$$

$$\Psi_{1,\uparrow}^\dagger \Psi_{2,\downarrow} \sim e^{i\sqrt{\pi}((V_\theta^{11}-V_\theta^{21})\tilde{\theta}_1+(V_\theta^{12}-V_\theta^{22})\tilde{\theta}_2)} e^{-i\sqrt{\pi}((V_\phi^{11}+V_\phi^{21})\tilde{\phi}_1+(V_\phi^{12}+V_\phi^{22})\tilde{\phi}_2)}. \tag{B3}$$

Calculating their scaling dimensions, we find that these terms are irrelevant (and can thus be omitted) if the following two conditions hold:

$$\frac{1}{4} \sum_{j=1,2} \left(V_\theta^{1j} - V_\theta^{2j} \right)^2 + \frac{1}{4} \sum_{j=1,2} \left(V_\phi^{1j} \mp V_\phi^{2j} \right)^2 > 1. \tag{B4}$$

Appendix C: Two-channel resonant-level model

In this section, we briefly discuss the solution of Eq. (24). We Fourier transform the Hamiltonian in this equation to cast it into a resonant-level model consisting of two non-interacting channels coupled to a discrete level modeled by d operators. The Hamiltonian becomes

$$H_{\text{T}} = \sum_{k,j} \epsilon_{k,j} c_{k,j}^\dagger c_{k,j} + \epsilon_d d^\dagger d + \sum_{k,J} t_j \left[c_{k,j}^\dagger d + c_{k,j} d^\dagger \right]. \tag{C1}$$

Here, $t_j = \frac{J_{\perp,j}}{\sqrt{4\pi^2\xi_j}}$ and $\epsilon_{k,j} = u_j k$. We look for new fermionic operators $f_n^\dagger = \sum_{k,j} M_{n,k}^j c_{k,j}^\dagger + L_n d^\dagger$ such that $H_{\rm T} = \sum_n E_n f_n^\dagger f_n + {\rm const}$. We then have $[H_{\rm T}, f_n^\dagger] = E_n f_n^\dagger$, and from Eq. (C1)

$$\left[H_{\rm T}, f_n^\dagger\right] = \sum_{k,j}[M_{n,k}^j \epsilon_{k,j} c_{k,j}^\dagger + t_j M_{n,k}^j d^\dagger + t_j L_n c_{k,j}^\dagger] + \epsilon_d L_n d^\dagger. \tag{C2}$$

We have used $[ab,c] = a\{b,c\} - \{a,c\}b$. Hence

$$E_n f_n^\dagger = \sum_{k,j}[M_{n,k}^j \epsilon_{k,j} c_{k,j}^\dagger + t_j M_{n,k}^j d^\dagger + t_j L_n c_{k,j}^\dagger] + \epsilon_d L_n d^\dagger,$$

$$E_n\left[\sum_{k,j} M_{n,k}^j c_{k,j}^\dagger + L_n d^\dagger\right] = \sum_{k,j}[M_{n,k}^j \epsilon_{k,j} c_{k,j}^\dagger + t_j L_n c_{k,j}^\dagger] + [\sum_{k,j} t_j M_{n,k}^j d^\dagger + \epsilon_d L_n d^\dagger]. \tag{C3}$$

If we introduce a resonant level coupled to a two independent channel set-up, then

$$E_n M_{n,k}^j = M_{n,k}^j \epsilon_{k,j} + t_j L_n,$$
$$E_n L_n = \sum_j t_j \sum_k M_{n,k}^j + \epsilon_d L_n. \tag{C4}$$

One would get

$$E_n = \sum_j t_j^2 \sum_k \frac{1}{E_n - \epsilon_{k,j}} + \epsilon_d. \tag{C5}$$

The above equation can be graphically solved for finite system [40]. We use the following relation [40] to evaluate the sum over k

$$\sum_{n=-\infty}^{\infty} \frac{1}{E_n - \pi n} = \cot(E_n). \tag{C6}$$

For $\epsilon_d = 0$

$$E_n = \sum_j \frac{\pi t_j^2}{u_j} \cot(\frac{E_n \pi}{u_j}). \tag{C7}$$

One can solve the above equation numerically to obtain the energy E_n. We can further derive the spectral function from the impurity Green's function. We note that in path integral formalism

$$Z = \int \mathcal{D}[d, c_j] e^{-S} = \int \mathcal{D}[d] e^{-S_d} \int \mathcal{D}[c] e^{-S_c},$$

$$S_d = \int_0^\beta d\tau \left[\bar{d}(\partial_\tau + \epsilon_d)d\right],$$

$$S_c = \sum_j \int_0^\beta d\tau \left[\sum_k \bar{c}_{k,j}(\partial_\tau + \epsilon_{k,j})c_{k,j} + \sum_k (t_j \bar{c}_{k,j} d + c_{k,j}\bar{d})\right]. \tag{C8}$$

From the above expressions we can write

$$Z = \int \mathcal{D}d e^{-\int_0^\beta d\tau \left[\bar{d}(\partial_\tau + \epsilon_d)d\right]} \int \mathcal{D}[c_1] e^{-\int_0^\beta d\tau \left[\sum_k \bar{c}_{k,1}(\partial_\tau + \epsilon_{k,1})c_{k,1} + \sum_k (t_\alpha \bar{c}_{k,1} d + c_{k,1}\bar{d})\right]}$$

$$\int \mathcal{D}[c_2] e^{-\int_0^\beta d\tau \left[\sum_k \bar{c}_{k,2}(\partial_\tau + \epsilon_{k,2})c_{k,2} + \sum_k (t_\alpha \bar{c}_{k,2} d + c_{k,2}\bar{d})\right]}. \tag{C9}$$

One can integrate out $c_{k,j}$'s to obtain

$$Z \sim \int \mathcal{D}d \exp\left[-\int_0^\beta d\tau \bar{d}(\partial_\tau + \epsilon_d - \sum_j \frac{t_j^2}{\partial_\tau + \epsilon_{k,j}})d\right]. \tag{C10}$$

Here we are showing the relevant term which depends on d operators. We next perform Fourier transformation $d(\tau) = \beta^{-1/2} \sum_n d_n e^{-i\omega_n \tau}$, where ω_n is n^{th} Matsubara frequency and β is inverse temperature. This enables us to replace ∂_τ by $-i\omega_n$.

$$Z \sim \int \mathcal{D}d \exp\left[-\sum_{i\omega_n} \bar{d}_n (-i\omega_n + \epsilon_d - \sum_j \frac{t_j^2}{-i\omega_n + \epsilon_{k,j}}) d_n \right]. \tag{C11}$$

Hence the impurity green's function can be written as

$$G_d(i\omega_n) = \frac{1}{i\omega_n - \epsilon_d + i\Gamma sgn(\omega_n)}. \tag{C12}$$

and the spectral function, defined as $-\frac{1}{\pi}\text{Im}(G_d)$, becomes a Lorentzian with width

$$\Gamma = \sum_j \Gamma_j = \sum_j \pi \frac{t_j^2}{u_j}. \tag{C13}$$

Appendix D: RG analysis

For completeness, in this appendix we provide the derivation of the flow equations for the Kondo couplings in the model (13) using the perturbative RG approach. (See, e.g., [41]). The (euclidean) action for the Kondo problem corresponding to the Hamiltonian (13) is $S = S_0 + S_K$, where

$$S_0 = \sum_{j=1,2} \int \frac{d\omega}{2\pi} |\omega| |\varphi_j(\omega)|^2, \tag{D1}$$

$$S_K = \sum_{j=1,2} \int d\tau \left[\frac{-i\tilde{J}'_{z,j}}{\sqrt{\pi}u_j} \partial_\tau \varphi_j \, \sigma^z + \frac{J_{\perp,j}}{2\pi\xi_j} \left(e^{i2\sqrt{\pi}\kappa_j\varphi_j} \sigma^+ + e^{-i2\sqrt{\pi}\kappa_j\varphi_j} \sigma^- \right) \right]. \tag{D2}$$

Here we use the notation $\varphi_j(\tau) \equiv \tilde{\phi}_j(0,\tau)$, and τ denotes imaginary time. Following [41] S_0 is obtained by integrating out $\varphi_j(x \neq 0, \tau)$. The action S contains a large frequency cutoff Λ, i.e., $|\omega| < \Lambda$ in all frequency integrations, where we identify $\Lambda = \frac{u_j}{\xi_j}$.

The RG approach proceeds as follows [41, 42]. We introduce a rescaled cutoff $\Lambda' = \Lambda/b$, where $b = e^l > 1$ is a scaling factor, with $\ell \ll 1$. We separate the field into slow and fast components, $\varphi_j = \varphi_j^< + \varphi_j^>$, where the first contains only frequency components smaller than Λ', and the latter contains frequency components between Λ' and Λ. We perform the same separation on $\vec{\sigma}$ as we do for the φ_j fields. We are using time-ordered bosonic correlation, hence for consistency of the calculation one has to use the time-ordered product of impurity spin as well. This is given by $\mathcal{T}[\sigma_<^\pm(\tau)\sigma_<^\mp(\tau')] = \frac{1}{2} + \sigma_<^z \text{sgn}(\tau - \tau')$ [41]. We then integrate over the fast component and obtain an effective action for the slow component, which has the same form as the original action, but with renormalized coefficients, from which we can read the RG equations.

After integrating out the fast modes, the effective action for the slow modes up to second order in the Kondo couplings takes the following expression:

$$S_{\text{eff}}[\varphi^<] = S_0[\varphi^<] + \langle S_K[\varphi]\rangle_> - \frac{1}{2}\left(\langle S_K^2[\varphi]\rangle_> - \langle S_K[\varphi]\rangle_>^2\right), \tag{D3}$$

where $\langle \ldots \rangle_>$ denotes the integration over the fast modes, i.e., using the action $S_0[\varphi^>]$. Let us begin with the calculation of the first-order correction. Here, we have used $\langle \partial_\tau \varphi_j\rangle_> = \partial_\tau \varphi_j^<$ and $\langle (\varphi_j^>)^2\rangle_> = \frac{1}{2\pi}\log b$. We now need to restore the cutoff to its original value Λ, which can be accomplished by rescaling the time $\tau \to b\tau$ and redefining the field $\varphi_j^<(\tau) \to \varphi_j^<(b\tau) \equiv \bar{\varphi}(\tau)$. Then we get

$$\langle S_K[\varphi]\rangle_> = \sum_j \int d\tau \left[\frac{-i\tilde{J}'_{z,j}}{\sqrt{\pi}u_j} \partial_\tau \bar{\varphi}_j \, \sigma^z + \frac{J_{\perp,j} b^{1-\kappa_j^2}}{2\pi\xi_j} \left(e^{i2\sqrt{\pi}\kappa_j\bar{\varphi}_j} \sigma^+ + e^{-i2\sqrt{\pi}\kappa_j\bar{\varphi}_j} \sigma^- \right) \right]. \tag{D4}$$

This results implies that $\tilde{J}'_{z,j}$ is not renormalized at first order, while for $J_{\perp,j}$ we find

$$\frac{dJ_{\perp,j}}{d\ell} = (1 - \kappa_j^2)J_{\perp,j}.$$

At the second order we find

$$\langle S_{\mathrm{K}}^2[\varphi]\rangle_> = \sum_{j_1,j_2} \int d\tau\, d\tau' \Big\langle \left[\frac{-i\tilde{J}'_{z,j_1}}{\sqrt{\pi}u_{j_1}} \partial_\tau \varphi_{j_1}(\tau)\sigma^z + \frac{J_{\perp,j_1}}{2\pi\xi_{j_1}} \left(e^{i2\sqrt{\pi}\kappa_{j_1}\varphi_{j_1}(\tau)}\sigma^+ + e^{-i2\sqrt{\pi}\kappa_{j_1}\varphi_{j_1}(\tau)}\sigma^- \right) \right] \times$$

$$\times \left[\frac{-i\tilde{J}'_{z,j_2}}{\sqrt{\pi}u_{j_2}} \partial_{\tau'} \varphi_{j_1}(\tau')\sigma^z + \frac{J_{\perp,j_2}}{2\pi\xi_{j_2}} \left(e^{i2\sqrt{\pi}\kappa_{j_2}\varphi_{j_2}(\tau')}\sigma^+ + e^{-i2\sqrt{\pi}\kappa_{j_2}\varphi_{j_2}(\tau')}\sigma^- \right) \right] \Big\rangle_>. \tag{D5}$$

We calculate only the quantity of interest:

$$\left\langle e^{i2s\sqrt{\pi}\kappa_j\varphi_j(\tau)} \partial_{\tau'}\varphi_j^>(\tau') \right\rangle_> = -\frac{2s\sqrt{\pi}}{ib^{\kappa_j}} e^{i2s\sqrt{\pi}\kappa_j\varphi_j^<(\tau)} \kappa_j \partial_{\tau'} \langle \varphi_j^>(\tau)\varphi_j^>(\tau')\rangle_>. \tag{D6}$$

Next, we make the change of variables $t = \tau - \tau'$ and $T = \frac{\tau+\tau'}{2}$, and Taylor-expand the fields around $t = 0$, so that they are only functions of the center of mass coordinate T. The t-integral is performed using a cut-off $1/\Lambda$. Collecting together the dominant terms, we obtain

$$\langle S_{\mathrm{K}}\rangle_> = \int dT \left[\frac{-i\tilde{J}'_{z,j}}{\sqrt{\pi}u_j} \partial_T \bar{\varphi}_j(T)\sigma^z + \frac{J_{\perp,j}}{2\pi\xi} \left(1 + (\kappa_j^2 - 1)\frac{\delta\Lambda}{\Lambda} \right) \left(e^{i2\sqrt{\pi}\kappa_j\bar{\varphi}_j(T)}\sigma^+ + e^{-i2\sqrt{\pi}\kappa_j\bar{\varphi}_j(T)}\sigma^- \right) \right],$$

$$-\frac{1}{2}(\langle S_{\mathrm{K}}^2\rangle_> - \langle S_{\mathrm{K}}\rangle_>^2) = \sum_{j=1}^2 \kappa_j \int dT \frac{J_{\perp,j}\tilde{J}'_{z,j}}{2\pi^2\xi_j u_j} \log b \left[e^{i2\sqrt{\pi}\kappa_j\varphi_j^<(T)}\sigma^+ + e^{-i2\sqrt{\pi}\kappa_j\varphi_j^<(T)}\sigma^- \right]$$

$$-\sum_{j=1}^2 \frac{(J_{\perp,j})^2}{(2\pi)^2\xi_j^2} 4\sqrt{\pi}\kappa_j^3 i\sigma^z \int dT \partial_T\varphi_j^<(T) \frac{1}{\Lambda^2} dl. \tag{D7}$$

We then arrive at the effective action with rescaled couplings

$$S_{\mathrm{eff}}[\bar{\varphi}] = S_0[\bar{\varphi}] + \int dT \left[\frac{-i\tilde{J}'_{z,j}(l)}{\sqrt{\pi}u_j} \partial_T \bar{\varphi}_j(T)\sigma^z + \frac{J_{\perp,j}(l)}{2\pi\xi_j} \left(e^{i2\sqrt{\pi}\kappa_j\bar{\varphi}_j(T)}\sigma^+ + e^{-i2\sqrt{\pi}\kappa_j\bar{\varphi}_j(T)}\sigma^- \right) \right]. \tag{D8}$$

where the couplings satisfy the following RG equations:

$$\frac{d\tilde{J}'_{z,j}}{dl} = \frac{\kappa_j^3}{\pi u_j}(J_{\perp,j})^2, \tag{D9}$$

$$\frac{dJ_{\perp,j}}{dl} = (1 - \kappa_j^2)J_{\perp,j} + \frac{\kappa_j}{\pi u_j}\tilde{J}'_{z,j}J_{\perp,j}. \tag{D10}$$

In terms of the unshifted couplings $\tilde{J}_{z,j}$, we find

$$\frac{d\tilde{J}_{z,j}}{dl} = \frac{\kappa_j^3}{\pi u_j}(J_{\perp,j})^2, \tag{D11}$$

$$\frac{dJ_{\perp,j}}{dl} = (1 - \kappa_j^2 - 2\kappa_j V_\phi^{\bar{j}j})J_{\perp,j} + \frac{\kappa_j}{\pi u_j}\tilde{J}_{z,j}J_{\perp,j},$$

$$= (1 - (V_\phi^{jj})^2 - (V_\phi^{\bar{j}j})^2)J_{\perp,j} + \frac{\kappa_j}{\pi u_j}\tilde{J}_{z,j}J_{\perp,j}. \tag{D12}$$

The first term in the last line can be easily understood: it is the scaling dimension of the $J_\perp$ operator in Eq. (11), after the diagonalization of the bulk Hamiltonian, but before any unitary transformation. In the limit of decoupled channels,

$$V_\phi^{ij} = \sqrt{K_j}\delta_{ij}, \quad V_\theta^{ij} = \delta_{ij}/\sqrt{K_j}, \quad \tilde{J}'_{z,j} = J_{z,j}/\sqrt{K_j}, \quad \kappa_j = \sqrt{K_j},$$

and we find

$$\frac{dJ_{z,j}}{dl} = \frac{K_j^2}{\pi u_j}(J_{\perp,j})^2, \tag{D13}$$

$$\frac{dJ_{\perp,j}}{dl} = (1 - K_j)J_{\perp,j} + \frac{1}{\pi u_j}J_{z,j}J_{\perp,j}. \tag{D14}$$

The equations differ from those in [18], which read

$$\frac{dJ_{z,j}}{dl} = \frac{1}{\pi u_j}(J_{\perp,j})^2, \tag{D15}$$

$$\frac{dJ_{\perp,j}}{dl} = (1 - K_j)J_{\perp,j} + \frac{1}{\pi u_j}J_{z,j}J_{\perp,j}. \tag{D16}$$

This can be understood as being due to the fact that the equations in [18] are only meant to be valid for weak e-e interactions, i.e., $K_j \approx 1$ (see comment in [41]).

We notice that the equation for $J_{\perp,j}$ can be easily obtained by using the Hamiltonian (15). Indeed, in this case we just need the scaling dimension of the $J_\perp$ operator:

$$\frac{dJ_{\perp,j}}{d\ell} = (1 - \sum_k \kappa_{jk}^2)J_{\perp,j}. \tag{D17}$$

We observe that

$$\sum_k \kappa_{jk}^2 = \sum_k \left(V_\phi^{jk} - \frac{\tilde{J}_{z,k}}{2\pi u_k} \right)^2 = \sum_k \left(V_\phi^{jk} - \frac{\tilde{J}'_{z,k}}{2\pi u_k} - V_\phi^{\bar{k}k} \right)^2, \tag{D18}$$

$$\approx \left(V_\phi^{jj} - V_\phi^{\bar{j}j} \right)^2 - \left(V_\phi^{jj} - V_\phi^{\bar{j}j} \right)^2 \frac{\tilde{J}'_{z,j}}{\pi u_j} = \kappa_j^2 - \frac{\kappa_j}{\pi u_j}\tilde{J}'_{z,j}. \tag{D19}$$

In the last line we used the definition of $\tilde{J}'_{z,j}$ in Eq. (14) and we omitted terms of order $\tilde{J}'^2_z$. Inserting this expression in Eq. (D17) we recover Eq. (D10).

Appendix E: Conductance for weak coupling

In this section we give some details of the calculation of the correction to the conductance at finite temperature and frequency. We start with the Hamiltonian $\tilde{H}$ in Eq. (15), which we rewrite here for convenience:

$$\tilde{H} = \sum_{j=1,2} \left[\frac{u_j}{2} \int dx \left[\tilde{\Pi}_j^2 + (\partial_x \tilde{\phi}_j)^2 \right] + \frac{J_{\perp,j}}{2\pi\xi_j} \left(e^{i2\sqrt{\pi}\sum_k \kappa_{jk}\tilde{\phi}_k(0)}\sigma^+ + \text{h.c.} \right) \right]. \tag{E1}$$

The spin flip current is given by $\delta I = -e\partial_t \sigma^z$ [19]. In our case this expression turns out to be

$$\delta I = ie \sum_{j=1,2} \frac{J_{\perp,j}}{2\pi\xi_j} \left[e^{i2\sqrt{\pi}\sum_k \kappa_{jk}\tilde{\phi}_k}\sigma^+ - e^{-i2\sqrt{\pi}\sum_k \kappa_{jk}\tilde{\phi}_k}\sigma^- \right]. \tag{E2}$$

The correction to the conductance $\delta\mathcal{G}(\omega)$ can be computed using the Kubo formula [21, 40], which amounts to calculating the current-current correlator from Eq. (E2) [19, 21]. For these calculations one needs to use the finite temperature bosonic correlators defined as [31, 32]

$$\langle \mathcal{T} \left[\tilde{\phi}_j(\tau) - \tilde{\phi}_j(0) \right]^2 \rangle = \frac{1}{2\pi} \log \left[\left(\frac{\beta u_j}{\pi\xi_j} \right)^2 \sin^2\left(\frac{\pi}{\beta}\tau \right) \right], \tag{E3}$$

where τ is imaginary time, $\beta = 1/T$, and $\xi_j = u_j/\Lambda$. We then obtain $\delta\mathcal{G}(\omega) = I_1 + I_2 + I_3$, where

$$I_1 = -2e^2 \left(\frac{J_{\perp,1}}{2\pi\xi_1} \right)^2 \left(\frac{\pi\xi_1}{\beta u_1} \right)^{2\kappa_{11}^2} \left(\frac{\pi\xi_2}{\beta u_2} \right)^{2\kappa_{12}^2} \sin\left(\pi(\kappa_{11}^2 + \kappa_{12}^2) \right) \int_0^\infty dt \frac{(e^{i\omega t} - 1)/i\omega}{|\sinh(\frac{\pi}{\beta}t)|^{2(\kappa_{11}^2 + \kappa_{12}^2)}},$$

$$I_2 = -2e^2 \left(\frac{J_{\perp,2}}{2\pi\xi_2} \right)^2 \left(\frac{\pi\xi_1}{\beta u_1} \right)^{2\kappa_{21}^2} \left(\frac{\pi\xi_2}{\beta u_2} \right)^{2\kappa_{22}^2} \sin\left(\pi(\kappa_{21}^2 + \kappa_{22}^2) \right) \int_0^\infty dt \frac{(e^{i\omega t} - 1)/i\omega}{|\sinh\left(\frac{\pi}{\beta}t \right)|^{2(\kappa_{21}^2 + \kappa_{22}^2)}}, \tag{E4}$$

$$I_3 = -4e^2 \frac{J_{\perp,1}J_{\perp,2}}{(2\pi)^2\xi_1\xi_2} \left(\frac{\pi\xi_1}{\beta u_1} \right)^{2(\kappa_{11}\kappa_{12})} \left(\frac{\pi\xi_2}{\beta u_2} \right)^{2\kappa_{22}\kappa_{21}} \sin\left(\pi(\kappa_{11}\kappa_{12} + \kappa_{22}\kappa_{21}) \right) \int_0^\infty dt \frac{(e^{i\omega t} - 1)/i\omega}{|\sinh\left(\frac{\pi}{\beta}t \right)|^{2(\kappa_{11}\kappa_{12} + \kappa_{22}\kappa_{21})}}.$$

In the limit $J_{\perp,j}^2 \ll \omega \ll T$ we can simplify the above expressions as follows:

$$
\begin{aligned}
I_1 &= -\frac{e^2}{4}\left(\frac{J_{\perp,1}}{2\pi\xi_1}\right)^2\left(\frac{2\pi T}{\Lambda}\right)^{2\kappa_{11}^2}\left(\frac{2\pi T}{\Lambda}\right)^{2\kappa_{12}^2}\left(\frac{1}{\pi T}\right)^2\frac{\pi\Gamma(\kappa_{11}^2+\kappa_{12}^2)^2}{\Gamma(2(\kappa_{11}^2+\kappa_{12}^2))}, \\
I_2 &= -\frac{e^2}{4}\left(\frac{J_{\perp,2}}{2\pi\xi_2}\right)^2\left(\frac{2\pi T}{\Lambda}\right)^{2\kappa_{21}^2}\left(\frac{2\pi T}{\Lambda}\right)^{2\kappa_{22}^2}\left(\frac{1}{\pi T}\right)^2\frac{\pi\Gamma(\kappa_{21}^2+\kappa_{22}^2)^2}{\Gamma(2(\kappa_{21}^2+\kappa_{22}^2))}, \\
I_3 &= -\frac{e^2}{2}\frac{J_{\perp,1}J_{\perp,2}}{(2\pi)^2\xi_1\xi_2}\left(\frac{2\pi T}{\Lambda}\right)^{2(\kappa_{11}\kappa_{12})}\left(\frac{2\pi T}{\Lambda}\right)^{2\kappa_{22}\kappa_{21}}\left(\frac{1}{\pi T}\right)^2\frac{\pi\Gamma(\kappa_{11}\kappa_{12}+\kappa_{22}\kappa_{21})^2}{\Gamma(2(\kappa_{11}\kappa_{12}+\kappa_{22}\kappa_{21}))}.
\end{aligned}
\tag{E5}
$$

The reduction of each of the integrals in Eq. (E4) to the three corresponding expressions in Eq. (E5) also depends on the fact that the terms $\kappa_{11}^2+\kappa_{12}^2, \kappa_{21}^2+\kappa_{22}^2, \kappa_{11}\kappa_{12}+\kappa_{22}\kappa_{21}$ are non-zero. One can observe from Eq. (E4) that these three terms correspond to I_1, I_2 and I_3 respectively. If any of these three quantities becomes zero, the corresponding integral goes to zero. We extend this argument to see from Eq. (E4) that I_3 vanishes in the exactly solvable limit. This shows that in this limit the correction takes the form of a sum of two contributions coming from two effectively independent channels, as in the case of the level width of the spectral function in Sec. III.

[1] F. D. M. Haldane, Phys. Rev. Lett. **61**, 2015 (1988).
[2] B. A. Bernevig, Topological Insulators and Topological Superconductors, Princeton: Princeton University Press (2013).
[3] M. Z. Hasan and C. L. Kane, Rev. Mod. Phys. **82**, 3045 (2010).
[4] C. L. Kane and E. J. Mele, Phys. Rev. Lett. **95**, 226801 (2005).
[5] C. L. Kane and E. J. Mele, Phys. Rev. Lett. **95**, 146802 (2005).
[6] B. A. Bernevig and S.-C. Zhang, Phys. Rev. Lett. **96**, 106802 (2006).
[7] C. Wu, B. A. Bernevig, and S.-C. Zhang, Phys. Rev. Lett. **96**, 106401 (2006).
[8] C. Xu and J. E. Moore, Phys. Rev. B **73**, 045322 (2006).
[9] Y. Tanaka and N. Nagaosa, Phys. Rev. Lett. **103**, 166403 (2009).
[10] P. W. Anderson, J. Phys. C **3**, 2436 (1970).
[11] P. Nozières and A. Blandin, J. Physique **41**, 193 (1980).
[12] M. Fabrizio, A. O. Gogolin, and P. Nozières, Phys. Rev. B **51**, 16088 (1995).
[13] P. Coleman and A. J. Schofield, Phys. Rev. Lett. **75**, 2184 (1995).
[14] D. L. Cox and A. Zawadowski, Adv. Phys. **47**, 599 (1998).
[15] A. C. Hewson, The Kondo Problem to Heavy Fermions, Cambridge University Press, Cambridge, UK (1993).
[16] A. Furusaki and N. Nagaosa, Phys. Rev. Lett. **72**, 892 (1994).
[17] A. Furusaki, J. Phys. Soc. Jpn. **74**, 73 (2005).
[18] J. Maciejko, C. Liu, Y. Oreg, X.-L. Qi, C. Wu, and S.-C. Zhang, Phys. Rev. Lett. **102**, 256803 (2009).
[19] Y. Tanaka, A. Furusaki, and K. A. Matveev, Phys. Rev. Lett. **106**, 236402 (2011).
[20] E. Eriksson, A. Ström, G. Sharma, and H. Johannesson, Phys. Rev. B **86**, 161103(R) (2012).
[21] E. Eriksson, Phys. Rev. B **87**, 235414 (2013).
[22] T. Posske, C.-X. Liu, J. C. Budich, and B. Trauzettel, Phys. Rev. Lett. **110**, 016602 (2013).
[23] T. Posske and B. Trauzettel, Phys. Rev. B **89**, 075108 (2014).
[24] K. T. Law, C. Y. Seng, P. A. Lee, and T. K. Ng, Phys. Rev. B **81**, 041305(R) (2010).
[25] Y.-L. Lee and Y.-W. Lee, Phys. Rev. B **88**, 035112 (2013).
[26] V. J. Emery and S. Kivelson, Phys. Rev. B **46**, 10812 (1992).
[27] G. Toulouse, C. R. Acad. Sci. Ser. B268, 1200 (1969).
[28] G. Zaránd and J. von Delft, Phys. Rev. B **61**, 6918 (2000).
[29] V. Kagalovsky, I. V. Lerner, and I. V. Yurkevich, Phys. Rev. B **95**, 205122 (2017).
[30] M. Jones, I. V. Lerner, and I. V. Yurkevich, Phys. Rev. B **96**, 174210 (2017).
[31] T. Giamarchi, Quantum Physics in One Dimension, Clarendon Press (London, 2004).
[32] E. Fradkin, Field Theories of Condensed Matter Physic, Cambridge University Press, (Cambridge, 2013).
[33] A. O. Gogolin, A.A. Nersesyan, A.M. Tsvelik, Bosonization and Strongly Correlated Systems, Cambridge University Press (Cambridge, 1998).
[34] I. V. Yurkevich, Europhys. Lett. **104**, 37004 (2013).
[35] I. V. Yurkevich and V. Kagalovsky, Sci. Rep. **11**, 18400 (2021).
[36] R. A. Santos, D. B. Gutman, and S. T. Carr, Phys. Rev. B **93**, 235436 (2016).
[37] V. Kagalovsky, A. L. Chudnovskiy, and I. V. Yurkevich, Phys. Rev. B **97**, 241116(R) (2018).
[38] A. M. Sengupta and A. Georges, Phys. Rev. B **49**, 10020 (1994).
[39] I. Affleck, Acta Phys. Polon. B **26**, 1869 (1995).
[40] P. Coleman, Introduction to Many-Body Physics, Cambridge University Press (2015).
[41] J. Maciejko, Phys. Rev. B **85**, 245108 (2012).
[42] A. Altland and B. D. Simons, Condensed matter Field Theory, Cambridge University Press (2010).
[43] R. Leturcq, L. Schmid, K. Ensslin, Y. Meir, D. C. Driscoll, and A. C. Gossard, Phys. Rev. Lett. **95**, 126603 (2005).

[44] J. Nygård, D. Cobden, and P. Lindelof, Nature **408**, 342 (2000).

[45] J. Martinek, M. Sindel, L. Borda, J. Barnaś, J. König, G. Schön, and J. von Delft, Phys. Rev. Lett. **91**, 247202 (2003).

[46] L. Kouwenhoven and L. Glazman, Phys. World 14, **33** (2001).